

SINGLE-FEED PLANAR ANTENNA FOR SUPPRESSING THE CHANGE IN RECEIVED SIGNAL LEVEL DUE TO STANDING WAVES IN MOBILE COMMUNICATION

H. H. Uchida

Graduate School of Science and Technology
Tokai University, 4-1-1 Kitakaname, Hiratsuka-Shi, Kanagawa, Japan

H. Matsui

DX Antenna Co., Ltd
2-15 Hamasaki-Dori, Hyogo-Ku, Kobe, Hyogo, Japan

O. Mikami

School of Engineering
Tokai University, 4-1-1 Kitakaname, Hiratsuka-Shi, Kanagawa, Japan

T. Wakabayashi

School of Information and Telecommunication Engineering
Tokai University, 2-3-23 Takanawa, Minato-ku, Tokyo, Japan

Abstract—The fading phenomenon resulting from standing waves is a factor in quality deterioration in mobile communication technologies (e.g., cellular phones and television receivers). Suppression of this fading phenomenon is needed for many kinds of technologies. A single-feed planar antenna composed of two antenna components, a Planar Monopole Antenna (PMA) and a Planar Slot Antenna (PSA), is proposed for reducing deterioration of reception due to the fading phenomenon. Reflection coefficient and radiation patterns are analyzed by the Finite Difference Time Domain (FDTD) method and compared with measured results. Results indicate that the proposed antenna has a resonant frequency with functions of the PMA and the PSA. The results of a field experiment at 583.76 MHz in the Ultra High Frequency (UHF) band indicate that the proposed antenna efficiently suppresses the fading phenomenon resulting from multipath propagation.

1. INTRODUCTION

Wireless applications have rapidly developed in mobile communications. Especially in broadcasting, many wireless systems that focus on reception with cellular phones and vehicles have been proposed and put to practical use, with the development of terrestrial digital TV.

Electromagnetic waves that are transmitted from a broadcasting station or cell tower interfere with waves reflected from buildings and form standing waves in urban areas bristling with buildings. Depending on the distribution of standing waves, changes in the received signal level (the fading phenomenon) occur. Due to the increasing transmission rates, communication quality suffers greatly, even though the fading phenomenon due to standing waves occurs quickly [1]. Thus, it is important to reduce the deterioration of reception quality in mobile communications due to this type of fading phenomenon.

With this goal, many researchers have studied various diversity technologies [2, 3]. Space diversity [4, 5] that arranges two or more antennas at spatially different positions alleviates the impact of the fading phenomenon due to standing waves. Also, polarization diversity [6, 7] can reduce the deterioration of reception quality by pairing antennas that have different polarizations. In standing waves, a phase difference of 90° exists between the electric field and the magnetic field. The maximum and minimum values of the electric field and the magnetic field appear alternately every quarter wavelength [1, 8]. Thus, a technique is proposed and gives useful characteristics, which an electric antenna and a magnetic antenna are combined by two feed points with a phase shifter and a combiner in order to receive electric and magnetic fields [9, 10]. These techniques are useful for reducing the deterioration of reception quality. However, they require plural feed points; therefore, the same number of feeding connectors and feeding cables as the number of feed points are required. They also require switching circuits that select and switch to the antenna with the highest level. These facts are a factor of increase in the cost of whole receiving system and block the miniaturization. Therefore, it is necessary to reduce the number of cables and eliminate electronic circuits for cost-saving, miniaturization, and weight-reduction.

A single-feed planar antenna composed of a planar monopole antenna (PMA) as an electric antenna and a planar slot antenna (PSA) as a magnetic antenna is thus proposed in order to reduce deterioration of the received signal level due to standing waves. The proposed antenna has the receiving function of a PMA that receives the standing wave of the electric field and that of a PSA that receives the standing

wave of the magnetic field, and suppresses changes in received signal level due to the fading phenomenon resulting from standing waves. Since it has a single-feed point [11, 13], it can improve reception quality without controlling phase and a switching circuit, a combiner, and a phase shifter. Also, production of the antenna is simple because the line element and conducting ground are printed on the same side of the dielectric substrate.

In this study, reflection coefficient, radiation patterns, and current distribution are first simulated by the Finite Difference Time Domain (FDTD) method [14]. Based on the simulated results, antennas are fabricated, and reflection coefficient and radiation patterns are measured and compared with the simulated results. A field experiment is then conducted at 583.76 MHz, which is the sound carrier frequency of a terrestrial TV broadcasting channel in Japan. The results indicate that the proposed antenna improves reception.

Section 2 discusses the structure of the proposed antenna, and Section 3 describes the simulation domain. Section 4 discusses the structures of the PMA and the PSA, which are components of the proposed antenna; simulated results of reflection coefficient, radiation patterns, and current distribution; and resonant mechanisms based on current distribution. It compares the reflection coefficient and the radiation patterns with the measured results. Section 5 discusses the composition of the proposed antenna and the resonant mechanism using current distribution. It also compares simulated reflection coefficient and radiation patterns with measured results. In addition, Section 6 discusses the method and results of the field experiment that was conducted to verify suppression of the fading phenomenon due to standing waves at Ultra High Frequency (UHF). Finally, Section 7 presents the conclusions.

2. STRUCTURE OF THE PROPOSED ANTENNA

The basic structure of the proposed antenna is illustrated in Figure 1. A similar idea of combination or radiators in a single port has been proposed using a slot and PIFA to obtain a multiband handset antenna [15]. Proposed antenna is composed of a PMA and a PSA. It has a line element and a conducting ground plane with a slot, which are printed on the same side of the dielectric substrate (relative permittivity: ϵ_r), which is $L_g + L_d$ in length, W_g in width, and h in thickness. The conducting ground is L_g in length and W_g in width. The line element is L in length and W in width.

The slot is L_s in length and W_s in width. The feed point placed on the same side of the conductors.

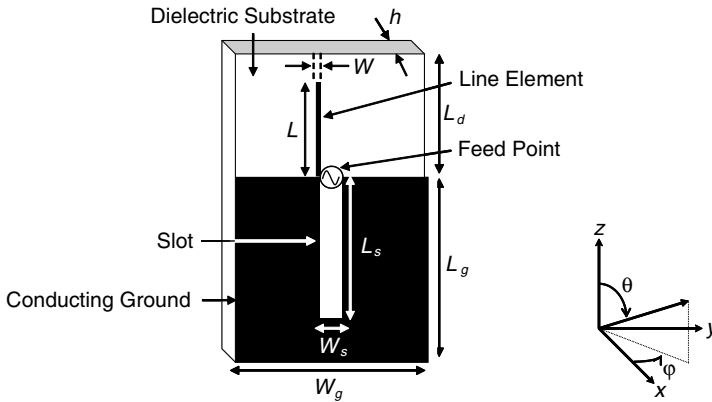


Figure 1. Structure of the proposed antenna.

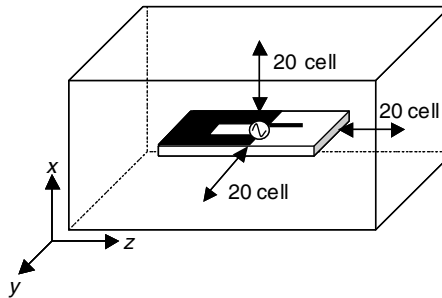


Figure 2. Simulation domain.

3. NUMERICAL METHOD

The PMA, the PSA, and the proposed antenna are analyzed by the FDTD method. With this method, the simulation domain is assumed as depicted in Figure 2. The distance between the antenna and the wall of the simulation domain in each direction is 20 cells. The cell size is $dx = dy = dz$. The input is a Gaussian pulse. A Perfectly Matched Layer (PML) is assumed as an eight-layer absorbing boundary in order to improve accuracy [16, 17]. Time step dt is determined by the following Courant stability condition:

$$dt \leq \frac{1}{c \sqrt{\left(\frac{1}{dx}\right)^2 + \left(\frac{1}{dy}\right)^2 + \left(\frac{1}{dz}\right)^2}}$$

where c is the velocity of wave propagation in vacuum.

4. COMPONENTS OF THE PROPOSED ANTENNA

This section describes the structures of the PMA and the PSA that are components of the proposed antenna, the simulated results, and a comparison with the measured results.

4.1. PMA and Its Characteristics

4.1.1. Simulated Results

The structure of the PMA that is used in the proposed antenna is depicted in Figure 3. The conducting ground and the line element are printed on the same side of the dielectric substrate, whose parameters are the same as those of the proposed antenna. Also, the feed point is placed on the same side.

The reflection coefficient of the PMA, whose line element width is $W = 1$ mm, is parameter L in Figure 4. The size of the dielectric substrate ($\epsilon_r = 7.35$) is $L_g + L_d = 270$, $L_g = W_g = 170$, and $h = 3$ mm. The resonant frequency of the PMA depends on the line element length L , and $L = 89$ mm corresponds to 583.76 MHz, which is desired for the field experiment. The current distribution at 583.76 MHz for $L = 89$ mm is presented in Figure 5. The dotted line represents a form of dielectric substrate, and the white parts on the conductors represent the magnitude of the current. The current distributes mostly on the line element, is strong at the base point (near the feed point), and is zero at the end portion. The length ($L = 89$ mm) is half of the element length of the basic planar dipole antenna, and the current distribution in Figure 5 is similar to that of the basic monopole

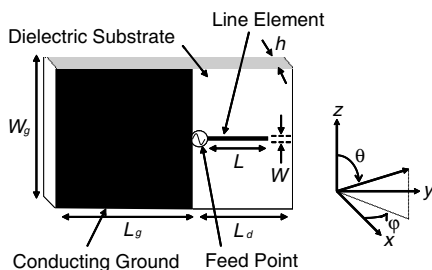


Figure 3. Structure of the PMA.

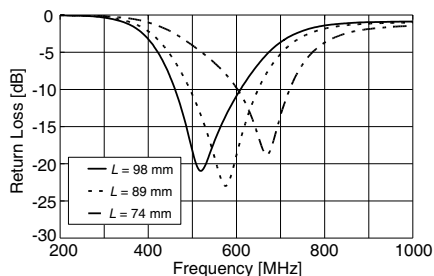


Figure 4. Reflection coefficient of the PMA for parameter L . $L_g = 170$, $W_g = 170$, $L_d = 100$, $L = 89$, $W = 1$, $h = 3$ mm, $\epsilon_r = 7.35$.

antenna [18, 19]. Therefore, it is clear that the PMA operates as a basic monopole antenna.

4.1.2. Measured Results

Based on the simulated results, a PMA with $L = 89$, $W = 1$, $L_g = W_g = 170$, and $L_d = 100$ mm shown in Figure 6 is fabricated in order to measure the reflection coefficient and conduct the field experiment. A glass substrate ($h = 3$ mm, $\varepsilon_r = 7.35$), which is used for car windows, was chosen as the dielectric substrate, and the PMA was connected to a coaxial cable through a $50\ \Omega$ system coaxial connector. Here, the core of the coaxial connector is soldered to the line element, and the outer conductor is soldered to the conducting ground. A vector network analyzer is used to measure the reflection coefficient.

Figure 7 compares simulated reflection coefficient and measured reflection coefficient when the length of the line element is 89 mm. The resonant frequency and the -10 dB bandwidth of the simulation correspond with the measured ones.

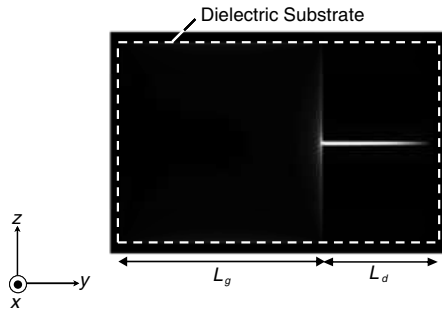


Figure 5. Current distribution of the PMA at 583.76 MHz.

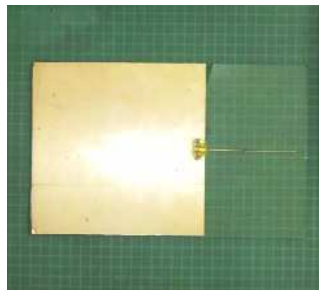


Figure 6. Fabricated PMA.

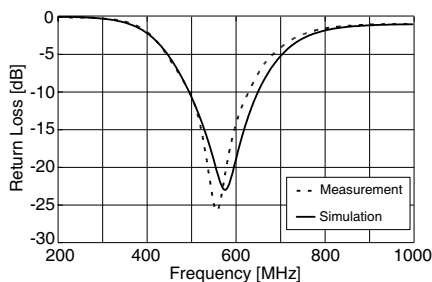


Figure 7. Reflection coefficient of the PMA. $L_g = 170$, $W_g = 170$, $L_d = 100$, $L = 89$, $W = 1$, $h = 3$ mm, $\epsilon_r = 7.35$.

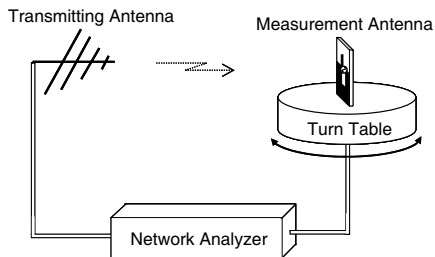


Figure 8. Measurement system of radiation patterns.

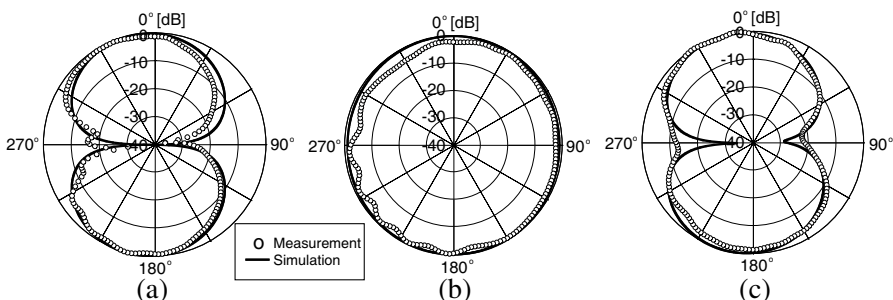


Figure 9. Co-polarized radiation patterns of the PMA at 583.76 MHz. (a) E_φ of xy -plane. (b) E_φ of xz -plane. (c) E_θ of zy -plane.

Figure 8 illustrates the radiation pattern measurement system. Radiation patterns in the xy -, xz -, and zy -planes were measured with a log periodic antenna as the transmitting antenna and a measured antenna on a turntable as the receiving antenna. This figure depicts the measurement system of the xy -plane as an example. In order to alleviate the effect of reradiation of current flowing on the coaxial cable, the coaxial cable was set along the rotary shaft of the turntable. Figure 9 presents the measured results of the radiation patterns of xy -, xz -, and zy -planes and the simulated results. Figures 9(a) and (b) provide the electric field component E_φ in the xy - and xz -planes, and Figure 8(c) provides E_θ in the zy -plane. Each figure is normalized by the maximum value of each characteristic. The measured results correspond well with simulated results in each plane. The measurement conditions of the reflection coefficient and radiation patterns with the coaxial cable and coaxial connector described above are the same as the following measurements.

4.2. PSA and Its Characteristics

4.2.1. Simulated Results

The structure of the PSA that is used in the proposed antenna is presented in Figure 10. The parameters of the slot, the conducting ground, and the dielectric substrate are the same as those of the proposed antenna depicted in Figure 1. The feed point is placed on the edge of the positive direction of z . The reflection coefficient of the PSA is presented as parameter L_s in Figure 11. The sizes of the dielectric substrate and the conducting ground are the same as those of the PMA. The resonant frequency of the PSA depends on the slot length L_s , and $L_s = 130$ mm corresponds to 583.76 MHz, which is the frequency desired for field experiment.

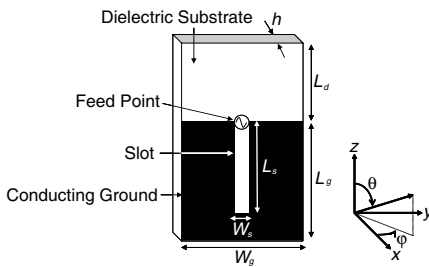


Figure 10. Structure of the PSA.

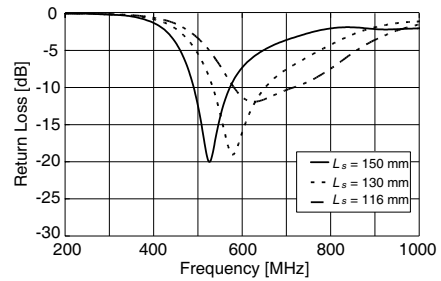


Figure 11. Reflection coefficient of the PSA for parameter L_s . $L_g = 170$, $W_g = 170$, $L_d = 100$, $W_s = 16$, $h = 3$ mm, $\varepsilon_r = 7.35$.

The current distribution at the resonant frequency for $L_s = 130$ mm is presented in Figure 12(a). The dotted line represents a form of the dielectric substrate, and the white parts around the slot represent the magnitude of the current on the conductor. Results indicate that the current distributes mostly around the edge of the slot. It is strong around both end portions (right and left end of the slot in Figure 12(a)) and weak at the central portion. Figure 12(b) presents a pattern diagram of current directions on the PSA. Currents on the edges around the central portion of the slot become weak because the upper and lower edge currents flow in opposite directions. As a result, the current around both ends of the slot become strong. A magnetic field is induced by the flow of the current described above, so that an electric field is induced, and electromagnetic waves radiate. Therefore, the PSA operates as an antenna with magnetic field detection.

4.2.2. Measured Results

Based on the simulated results, a PSA with a slot of $L_s = 130$ and $W_s = 16$ mm shown in Figure 13 is fabricated in order to measure the reflection coefficient and use in the field experiment. The conducting ground and the dielectric substrate ($h = 3$ mm, $\epsilon_r = 7.35$) are the same size as those of the PMA. The antenna was connected to a coaxial cable through a $50\ \Omega$ system coaxial connector. Here, the core of the coaxial connector is soldered to the right side of the conducting ground (positive direction of y), and the outer conductor is soldered to the left side of the conducting ground (negative direction of y) (Figure 9).

Figure 14 compares the simulated reflection coefficient and the measured reflection coefficient when the slot is 130 mm long. The

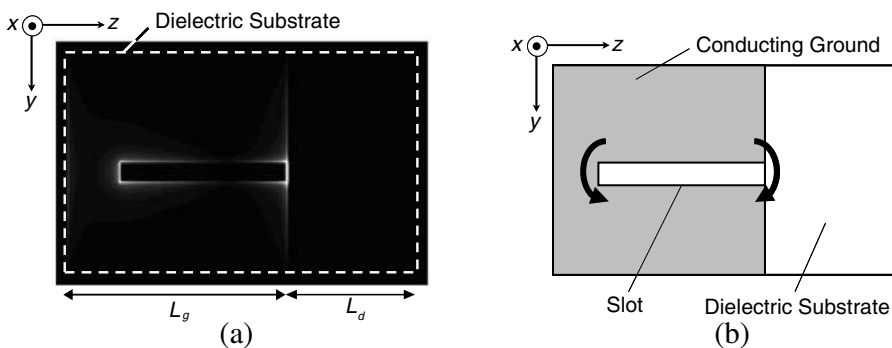


Figure 12. Current distribution and pattern diagram of the PSA. (a) Current distribution at 583.76 MHz. (b) Pattern diagram.

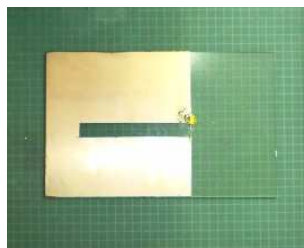


Figure 13. Fabricated PSA.

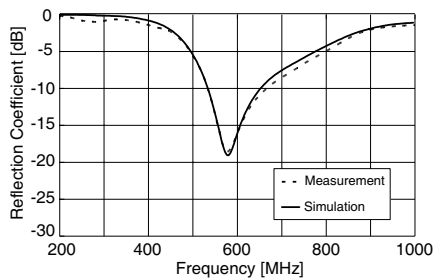


Figure 14. Reflection coefficient of the PSA. $L_g = 170$, $W_g = 170$, $L_d = 100$, $L_s = 130$, $W_s = 16$, $h = 3$ mm, $\epsilon_r = 7.35$.

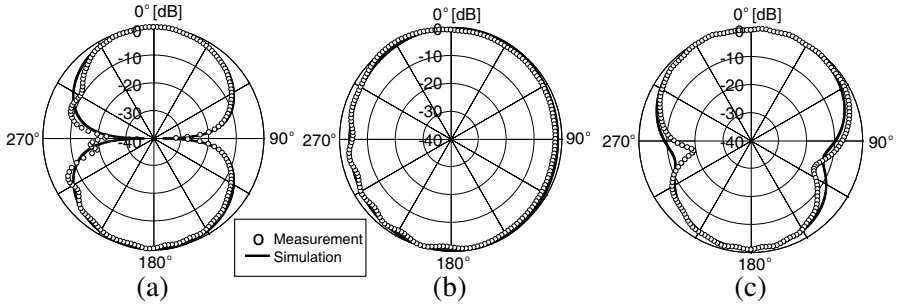


Figure 15. Co-polarized radiation patterns of the PSA at 583.76 MHz. (a) E_φ of xy -plane. (b) E_φ of xz -plane. (c) E_θ of zy -plane.

resonant frequency and the -10 dB bandwidth of the simulation correspond well with the measured ones. Figure 15 presents the measured results of the radiation patterns of the xy -, xz -, and zy -planes with the simulated results. These figures present the co-polarized electric field component E_φ in the xy - and xz -planes, and E_θ in the zy -plane. The figures are normalized by the maximum value of the characteristics. The measured results correspond well with the simulated results in each plane.

5. PROPOSED ANTENNA AND ITS CHARACTERISTICS

5.1. Composition

The proposed antenna, which combines a PMA with electric field detection and a PSA with magnetic field detection, is fabricated as follows.

- (1) The target frequency (583.76 MHz) is set.
- (2) Parameters are chosen (Figure 1) as $L_g = W_g = 170$, $L_g + L_d = 270$, $h = 3$ mm, $\varepsilon_r = 7.35$; the size of the line element is $L = 69$ and $W = 1$ mm; and the size of the slot is $L_s = 130$ and $W_s = 16$ mm, so as to resonate at the target frequency.
- (3) The resonant frequency of the proposed antenna is adjusted by changing the size of the slot or the length of the line element. Practically, the frequency 583.76 MHz was adjusted by shortening the length of the line element without changing the size of the slot. It is $L = 69$ mm at this point.

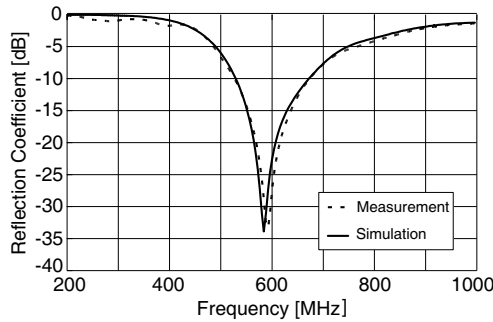


Figure 16. Reflection coefficient of the proposed antenna. $L_g = 170$, $W_g = 170$, $L_d = 100$, $L = 69$, $W = 1$, $L_s = 130$, $W_s = 16$, $h = 3$ mm, $\epsilon_r = 7.35$.

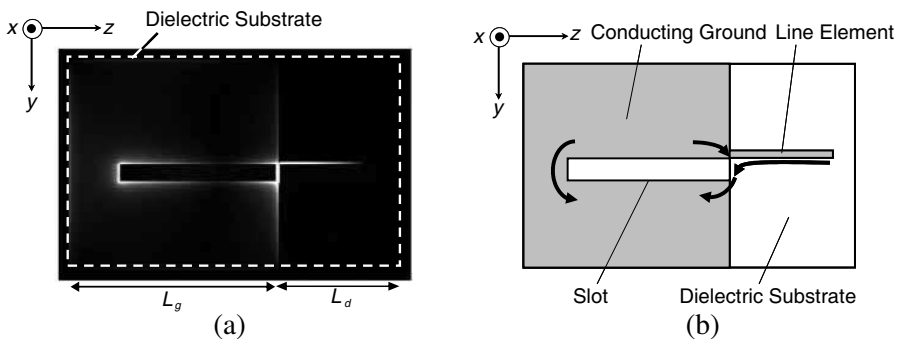


Figure 17. Current distribution and pattern diagram of the proposed antenna. (a) Current distribution at 583.76 MHz. (b) Pattern diagram.

5.2. Characteristics

5.2.1. Simulated Results

The solid line in Figure 16 denotes the simulated reflection coefficient of the proposed antenna. The proposed antenna resonates at the target frequency, and its -10 dB relative bandwidth is 23.3%. The current distribution at the resonant frequency is presented in Figure 17(a). The dotted line represents the form of the dielectric substrate. The line element is placed on the right side of the substrate, and the slot is loaded in the conducting ground placed on the left side of the substrate. In the figure, the white parts on the line element and around the slot represent the current distribution. Figure 17(a) indicates that

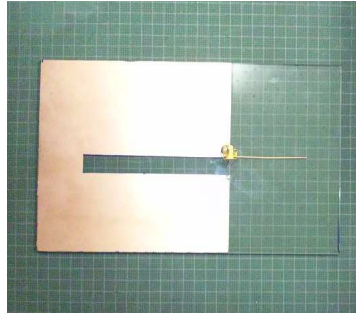


Figure 18. Fabricated proposed antenna.

the tendency of the current distribution on both the line element and the slot is the same as that on the PMA and the PSA in Figures 5 and 12(a). Thus the proposed antenna retains the functions of both the PMA and the PSA, even though these components are combined with a single-feed point.

Figure 17(b) is a pattern diagram of the current directions on the proposed antenna. The proposed antenna induces an electric field by the flow of the current on the line element, and a magnetic field by the flow of the current around the slot. Since the proposed antenna is a single-feed structure, the current is synthesized for reception without adjusting the phase.

For reception of the standing waves, a phase difference of 90° exists between the electric field and the magnetic field. Where the electric field becomes maximum, the magnetic field becomes minimum. Conversely, where the electric field becomes minimum, the magnetic field becomes maximum. Thus, their distributions are mutually compensating [1]. A system with only an antenna that maximum, the magnetic field becomes minimum. Conversely, where the electric field becomes minimum, the magnetic field becomes maximum. Thus, their distributions are mutually compensating [1]. A system with only an antenna that has electric field detection, suffers the fading phenomenon as the electric field changes. However, the proposed antenna has a line element that operates as a PMA with electric field detection, as well as a slot that operates as a PSA with magnetic field detection. Currents that are induced by both fields are synthesized at the feed point. Therefore, when the electric field becomes minimum, the proposed antenna detects the magnetic field, and change in the received signal level due to the fading phenomenon is suppressed.

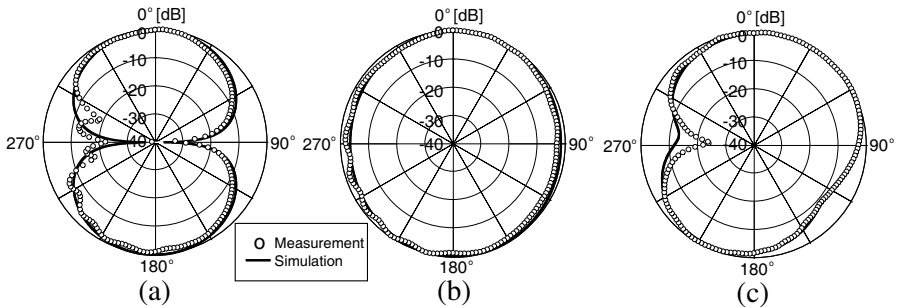


Figure 19. Co-polarized radiation patterns of the proposed antenna at 583.76 MHz. (a) E_φ of xy -plane. (b) E_φ of xz -plane. (c) E_θ of zy -plane.

5.2.2. Measured Results

The proposed antenna ($L = 69$, $W = 1$, $L_s = 130$, $W_s = 16$, $L_g = W_g = 170$, $L_g + L_d = 270$ mm) is fabricated as shown in Figure 18. A glass substrate ($h = 3$ mm, $\epsilon_r = 7.35$) is used for the dielectric substrate. At the feed point (Figure 1), the cable core of the coaxial connector is soldered to the right side of the conducting ground (positive direction of y), and the outer conductor is soldered to the left side of the conducting ground (negative side of y). Figure 16 compares the measured reflection coefficient and the simulated reflection coefficient. The resonant frequency and the -10 dB bandwidth of the simulation agree well with those of the measurement.

The radiation patterns of the xy -, xz -, and zy -planes are depicted with the measured results in Figure 19. It provides the co-polarized electric field component E_φ in xy - and xz -planes, and E_θ in the zy -plane. The figures are normalized by the maximum characteristics. In Figure 19(c), a decline in sensitivity can be seen in the 270° direction, as a result of the radiation pattern of the PSA depicted in Figure 15(c). The measured results in Figures 19(a) and (b) correspond well with the simulated results.

6. FIELD EXPERIMENT

In order to verify that the proposed antenna reduces quality deterioration due to fading resulting from standing waves, a field experiment was executed using a PMA, a PSA, and the proposed antenna. This section discusses the field experiment system and its results.

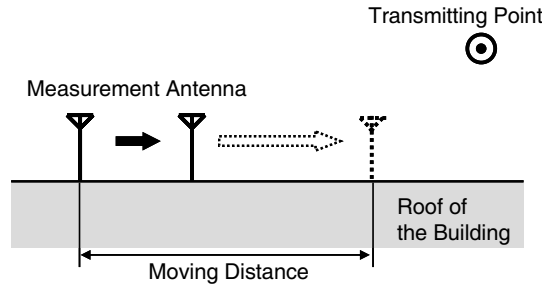


Figure 20. Measuring method of field experiment.

6.1. Field Experiment System

The target frequency is 583.76 MHz, which is the sound carrier frequency of a Japanese terrestrial broadcasting channel. It is transmitted vertically polarized from a relay station at 1 kW. Figure 20 depicts the experiment system at the receiving point 5 km from the transmitting point. The receiving point is a sufficiently large roof of a building, and the moving route (measurement route) is set as it parallels to a wall that generates standing waves. Here, the transmitting point on the right side of the figure is 45° from the measuring route. Measuring antennas are placed on a 2.0 m high tripod set up on a carriage moving along the measurement route. The height is set at 2.0 m because that was the height at which the strongest signal was received in a preliminary measurement. The proposed antenna was set as a line element pointed in the vertical direction, in order to receive the vertically polarized electric field; the edge of the conducting ground plane was directed toward the relay station in order to receive the magnetic field with the slot. Also, a wooden tripod and a wooden carriage were chosen in order to prevent their influence on reception.

To measure the received signal level, the PMA, PSA, and proposed antenna were moved in the same direction along the same moving route and the detected signal was measured by a spectrum analyzer.

6.2. Results of Field Experiment

The results of this field experiment are specified in Figure 21. The received signal levels are normalized by a maximum value of those characteristics.

Both the PMA and the PSA change greatly in received signal level, depending on where a standing wave is formed in the field. Distances between the minima of each standing wave are about 360 mm and 355 mm, which is about 1.4 times half of the transmitting wavelength.

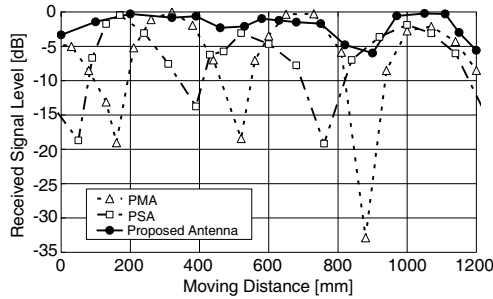


Figure 21. Measurement results of received signal level at 583.76 MHz.

Because the moving direction of the transmitting waves and the measurement route angle is about 45° . The maximum signal levels of the PMA and the PSA appear alternately; the maximum signal level of the PSA is detected near the minimum signal level of the PMA, and the maximum signal level of the PMA is detected near the minimum signal level of the PSA. However, the received signal level of the proposed antenna changes less than those of the PMA and the PSA and almost compensates for the decrease in the received signal level of the components. The range of change is 5.41 dB at most; therefore, the change is about $1/6$ of that with the PMA and $1/4$ of that with the PSA.

The following three conclusions are based on these results.

- (1) The PMA receives electric field standing waves, and the PSA receives magnetic field standing waves.
- (2) Maximum signal levels appear alternately between the received signal levels of the PMA and those of the PSA and compensate for minimum signal levels.
- (3) The proposed antenna receives both electric and magnetic field standing waves, and the composite received signal level changes much less than signals of the PMA and the PSA.

These results correspond with an experiment result of a small antenna designed for electric and magnetic field reception [10] and composed of a dipole antenna and a slot antenna with two feed points using a phase shifter and a combiner. It is thus evident that the proposed antenna, which is composed of a PMA and a PSA with a single-feed structure, reduces deterioration of the received signal level due to fading resulting from standing waves. The proposed antenna's ability to improve the signal level without using a phase shifter, a combiner, a switching circuit is a great advantage.

7. CONCLUSIONS

A single-feed planar antenna composed of two antenna components, a planar monopole antenna (PMA) and a planar slot antenna (PSA), was proposed to reduce deterioration of reception quality by fading due to standing waves.

Reflection coefficient, current distributions and radiation patterns of the components (PMA and PSA) were analyzed by the FDTD method. Their resonant mechanisms were revealed, based on reflection coefficient and current distribution. The antennas were fabricated, and their characteristics were measured. The simulated results corresponded well with the measured results.

The proposed antenna was then composed and analyzed. Based on the reflection coefficient and current distribution of the simulation, the resonant mechanism of the antenna was determined. It was fabricated and the characteristics were measured. The simulated results corresponded well with the measured results, and the fact that the proposed antenna has a resonant frequency with the functions of the PMA and the PSA was revealed numerically and experimentally.

A field experiment was conducted to verify the antenna's ability to reduce quality deterioration due to fading resulting from standing waves. The experiment measured the reception of the proposed antenna and its two components (a PMA and a PSA). Although the received signal levels of the PMA and the PSA changed significantly because of the reception of standing waves, the change in the signal level of the proposed antenna was much smaller and the receiving pattern covered the maximum levels of the components. Moreover, the experiment verified that the proposed antenna reduced deterioration of the received signal level by a single-feed structure without using a phase shifter, a combiner, or a switching circuit. Therefore, the proposed antenna is useful for reducing received signal deterioration due to fading resulting from standing waves in mobile communications.

In the near future, a broadband version of the proposed antenna for terrestrial digital TV will be investigated.

REFERENCES

1. Ito, K. and S. Sasaki, "A small printed receiving antenna for indoor communications," *IEICE Journal*, Vol. 71, No. 11, 1368–1369, Nov. 1988.
2. Yoshida, S. and N. Nakajima, "Antennas and propagation," *IEICE Journal*, Vol. 68, No. 11, 1232–1238, Nov. 1985.
3. Li, H.-J., T.-Y. Liu, and J.-L. Leou, "Antenna measurements in

- the presence of multipath waves,” *Progress In Electromagnetics Research*, Vol. 30, 157–178, 2001.
4. Jakes, Jr., W. C., “A comparison of specific space diversity techniques for reduction of fast fading in UHF mobile radio systems,” *IEEE Transactions on Vehicular Technology*, Vol. 20, No. 4, 81–92, Nov. 1971.
 5. Lee, W. C.-Y., “Antenna spacing requirement for a mobile radio base-station diversity,” *The Bell System Technical Journal*, Vol. 50, No. 6, 1859–1876, Jul.–Aug. 1971.
 6. Lee, W. C.-Y. and Y. S. Yeh, “Polarization diversity system for mobile radio,” *IEEE Transactions on Communication*, Vol. 20, No. 5, 912–923, Oct. 1972.
 7. Tu, T.-C., C.-M. Li, and C.-C. Chiu, “The performance of polarization diversity schemes in outdoor micro cells,” *Progress In Electromagnetics Research*, Vol. 55, 175–188, 2005.
 8. Harrington, R. F., *Time-harmonic Electromagnetic Fields*, McGraw-Hill Book Company, Inc., 1961.
 9. Hong, Z., H. Fujiwara, K. Okada, and K. Ito, “Small antenna aiming at electric and magnetic field reception for mobile communications in cities,” *ITE Technical Report*, Vol. 29, No. 15, 21–24, Feb. 2005.
 10. Hong, Z., H. Fujiwara, K. Okada, and K. Ito, “Antenna composed of printed dipole and slot for reception of electric and magnetic fields,” *Proceedings of IEICE General Conference 2005*, Vol. 55, 55, Mar. 2005.
 11. Uchida, H. H., H. Matsui, and T. Wakabayashi, “Single-feed planar antenna for electric and magnetic fields reception,” *Proc. of 2008 IEEE International Symposium on Antennas & Propagation*, 313.9, Jul. 2008.
 12. Uchida, H. H., H. Matsui, and T. Wakabayashi, “Characteristics of single-feed planar antenna for improvement of fading phenomenon,” *Proc. of 2009 IEEE International Symposium on Antennas & Propagation*, 211.8, Jun. 2009.
 13. Uchida, H. H., H. Matsui, and T. Wakabayashi, “Measurement of a single-feed planar antenna for improvement of fading phenomenon,” *Proc. of ISCIT 2009*, 6A-2, Sep. 2009.
 14. Uno, T., *Finite Difference Time Domain Method for Electromagnetic Field and Antennas*, Corona Publishing Co., Ltd., Tokyo, 1998.
 15. Anguera, J., I. Sanz, J. Mumburu, and C. Puente, “Multi-band handset antenna with a parallel excitation of PIFA and slot

- radiators”, *IEEE Transactions on Antennas and Propagation*, Vol. 58, No. 2, 348–356, Feb. 2010.
16. Kokubo, R., H. Matsui, and T. Wakabayashi, “Consideration of analytical parameters in FDTD method for planar antenna analysis,” *Proc. of 2006 KJJC, EMT-4-12*, 417–420, Sep. 2006.
 17. Niikura, K., R. Kokubo, K. Southisombath, H. Matsui, and T. Wakabayashi, “On analysis of planar antennas using FDTD method,” *PIERS Proceedings*, 1113–1117, Beijing, China, Mar. 26–30, 2007.
 18. Matsui, H. and T. Wakabayashi, “Single-feed planar antennas with three-frequency bands printed on the dielectric substrate and their applications,” *Journal of ITE*, Vol. 62, No. 1, 92–101, 2008.
 19. Matsui, H. and T. Wakabayashi, “Broadbanding of a planar antenna with three frequency bands and its application,” *ETRI Journal*, Vol. 29, No. 6, 725–735, 2007.